



Design and Properties of Advanced γ (TiAl) Alloys

Fritz Appel, Helmut Clemens and Michael Oehring

Institute for Materials Research, GKSS Research Centre,
Max-Planck-Str., D-21502 Geesthacht, GERMANY

Summary

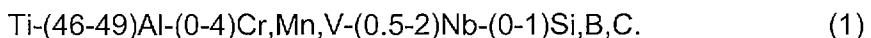
Intermetallic titanium aluminides are one of the few classes of emerging materials that have the potential to be used in demanding high-temperature structural applications whenever specific strength and stiffness are of major concern. However, in order to effectively replace the heavier nickel-base superalloys currently in use, titanium aluminides must combine a wide range of mechanical property capabilities. Advanced alloy designs are tailored for strength, toughness, creep resistance, and environmental stability. Some of these concerns are addressed in the present paper through global commentary on the physical metallurgy and technology of gamma TiAl-base alloys. Particular emphasis is paid on recent developments of TiAl alloys with enhanced high-temperature capability.

Keywords

Intermetallic titanium aluminides, failure mechanisms, properties, processing

1. Introduction

Titanium aluminide alloys exhibit unique mechanical properties combined with low density and good oxidation and ignition resistance. Thus, they are one of the few classes of emerging materials that have the potential to be used in demanding structural applications at elevated temperatures and in hostile environments. A vast amount of efforts has been expended over the past ten years in attempts to optimize the composition and microstructure of the alloys [1-5]. These have led to complex alloys with the general composition (in at.%)



The major phases in alloys of this type are $\gamma(\text{TiAl})$ and $\alpha_2(\text{Ti}_3\text{Al})$. In general, a reduction of Al content tends to increase the strength level, but is harmful for ductility and oxidation resistance. Additions of Cr, Mn and V up to levels of 2 % for each element have been shown to enhance ductility. The role of various other third elements is to improve other desired properties such as oxidation resistance (Nb, Ta) and creep strength (W, Mo, Si, C) [1]. Boron additions greater than 0.5 at.% are effective in refining the grain size and stabilizing the microstructure [6]. The addition of third elements not only changes the relative stability and transformation pathways of the phases, but also brings new phases into existence. It must be mentioned that the full details of the high-temperature phase equilibria and sequence of phase evolution with temperature and ternary or higher additions are not yet fully understood. By thermomechanical treatments a broad variety of microstructures can be generated in the alloys described by (1), which are often characterized in terms of the volume fraction of lamellar colonies and equiaxed γ grains; these are fully-lamellar, nearly-lamellar, duplex and near gamma structures. The general features of the correlations between alloy chemistry, microstructure and properties have been outlined in various review papers which should be consulted for additional background and information [1-6]. The established database indicates that the alloys are viable materials for engineering applications [7]. However, in spite of the potential technological impact of $\gamma(\text{TiAl})$ -base alloys, the useful range of application is limited by their susceptibility to brittle fracture, which persists up to 700 °C and the rapid loss of strength at higher temperature. Thus, in most mechanical properties the titanium aluminides are inferior to the nickel-base superalloys currently in use, even if the comparison is made on a strength to weight basis. This impedes practical use of the titanium aluminides and is the driving force for the current research and development.

As with many other materials, the alloy attributes that are desirable for high temperature service are counter to those that are considered to be desirable for low temperature toughness and damage tolerance. Thus, the balance of the mechanical properties has to be carefully chosen by the alloy design. This needs a detailed understanding of the relevant failure processes and their correlation with alloy chemistry and microstructure. At the same time, the capability for the alloy design is strongly related to the constraints of acceptable processing routes. These concerns are addressed in the present paper through global commentary on the physical metallurgy of $\gamma(\text{TiAl})$ -base alloys and the associated processing technologies. Particular emphasis is paid on recent developments of TiAl alloys with enhanced high temperature capabil-

ity. In order to limit the scope of this review, consideration will be given in separate sections to the following topics:

- deformation behaviour, dislocation multiplication and mobilities,
- creep properties,
- implementation of strengthening mechanisms,
- processing.

2. Deformation Behaviour:

Titanium aluminides are relatively brittle materials, exhibiting little plasticity at ambient temperatures. Typical of such deformation behaviour is that the gliding dislocations are either too low in density or too immobile to allow the specimen to match the superimposed strain rate. At elevated temperatures titanium aluminides suffer from insufficient creep resistance and structural changes. Such behaviour is often associated with dislocation climb and the operation of diffusion assisted dislocation sources [3]. Thus, the factors governing the multiplication and mobility of the dislocations might be important in several different ways and will now be considered.

2.1 Generation of perfect and twinning partial dislocations:

In two-phase alloys deformation of the $\gamma(\text{TiAl})$ phase is mainly provided by ordinary dislocations with Burgers vector $b = 1/2\langle 110 \rangle$ and order twinning $1/6\langle 11\bar{2} \rangle\{111\}$ [3, 8]. Ordinary $1/2\langle 110 \rangle$ dislocations have a compact core structure [9], which suggests that cross slip and climb are relatively easy. Multiplication of these dislocations can therefore take place through the operation of dislocation sources incorporating stress driven cross slip or climb as has been observed in disordered metals [10]. At room temperature multiplication has been found to be closely related to jogs in screw dislocations, which were probably generated by cross slip (figure 1a) [3, 11].

At elevated temperatures multiplication of ordinary dislocations occurs through the operation of Bardeen-Herring climb sources [3] as demonstrated in figure 1b by a sequence of micrographs, part of a TEM in situ study. Apparently, the critical vacancy concentration required to operate a Bardeen-

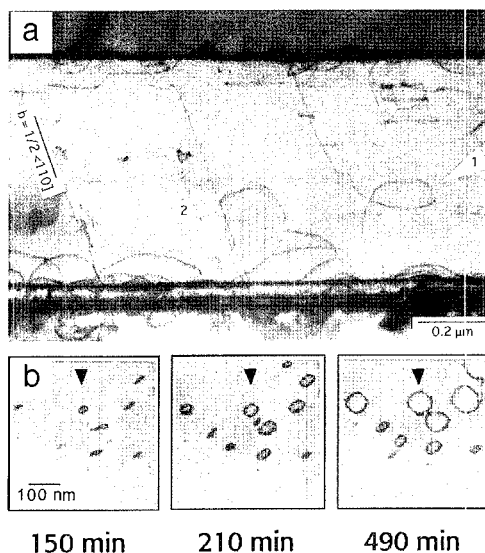


Figure 1. Dislocation generation in a two-phase titanium aluminide alloy of composition Ti-48Al-2Cr. (a) Initial stage of multiplication of an ordinary $1/2\langle 110 \rangle$ dislocation by cross glide. The dipole arms trailed at a high jog (1) in a screw dislocation are widely separated so that they could pass each other and may act as single ended dislocation sources. Note the emission of the dislocation loops (2) from the interface, which have been discussed in the text. Compression at $T = 300$ K to strain $\varepsilon = 3\%$. (b) Nucleation and growth of prismatic dislocation loops during in situ heating inside the TEM, following predeformation of the sample at room temperature to strain $\varepsilon = 3\%$.

Herring source is relatively low. Processing routes of titanium aluminides often involve thermal treatments followed by rapid cooling, which certainly leads to large vacancy supersaturations. Under such conditions Bardeen-Herring sources can probably operate throughout the entire period where annealing out of excess vacancies takes place.

A mechanism common to both low and elevated temperatures is the emission of ordinary dislocations from the mismatch structures of lamellar interfaces, which is certainly supported by coherency stresses [3, 11-14]. As with many other materials, twins in $\gamma(\text{TiAl})$ preferentially nucleate at lattice defects with a favorable atomic configuration, which can be rearranged into an embryonic

twin [15]. In two-phase titanium aluminides the lamellar interfaces seem to be the prevalent sites for twin formation. The twins are nucleated at misfit dislocations with a Burgers vector out of the interfacial phase which provide a Burgers vector component parallel to the twinning shear direction [15]. There are one-plane ledges in the twin/matrix interface, suggesting that the twins have grown through the propagation of Shockley partial dislocations.

The relative contributions of dislocation glide and twinning depends on the aluminium concentration, the content of ternary and quaternary elements, and the deformation conditions. There is growing evidence that the activation of superdislocations in the $\gamma(\text{TiAl})$ phase of two-phase alloys requires significantly higher shear stresses so that the different dislocation glide systems often cannot simultaneously operate. Thus, there are many more restrictions upon possible deformation modes in $\gamma(\text{TiAl})$ than for disordered metals with face centered cubic structures. In grains or lamellae which are unfavorably oriented for $1/2\langle 110 \rangle$ glide or twinning, significant constraint stresses can be developed due to the shape change of deformed adjacent grains. It is now well established that $\gamma(\text{TiAl})$ is prone to cleavage fracture on $\{111\}$ planes [11, 16, 17], which at the same time are the glide planes and twin habit planes. Thus, blocked dislocation glide and twinning may easily lead to the nucleation of cracks. Once nucleated on $\{111\}$ planes, the cracks can rapidly grow to a critical length. For an alloy design towards improved ductility, thus, the activation of glide involving c-components of the tetragonal unit cell of $\gamma(\text{TiAl})$ is of major concern.

2.2 Dislocation mobilities:

Information about the factors governing the dislocation mobility in $\alpha_2(\text{Ti}_3\text{Al}) + \gamma(\text{TiAl})$ alloys have been obtained by TEM observations and analyzing the deformation behaviour in terms of thermodynamic glide parameters. When the effects of temperature T and strain rate $\dot{\epsilon}$ are coupled by an Arrhenius type equation, the total flow stress σ can be described as [18-20]

$$\sigma = \sigma_{\mu} + \sigma^* = \sigma_{\mu} + (f/V) (\Delta F^* + kT \ln \dot{\epsilon}/\dot{\epsilon}_0), \quad (2)$$

with

$$\Delta F^* = \Delta G + V\sigma^*/f. \quad (3)$$

σ_{μ} is the long-range internal stress, σ^* is the thermal stress part and V is the activation volume. ΔF^* is the free energy and ΔG the Gibbs free energy of activation. γ_0 is considered to be constant, k is the Boltzmann constant and $f = 3.06$ is a Taylor factor to convert σ and γ to average shear quantities. The activation parameters V , ΔG and ΔF^* involved in eqs. 2 and 3 were determined by strain rate and temperature cycling tests according to the method proposed by Schöck [18]. V can be described as the number of atoms that have to be coherently thermally activated for overcoming the glide obstacles by the dislocations. It is therefore expected that V will undergo a significant change when there is a change of the mechanism that controls the glide resistance of the dislocations. The characteristic temperature dependence of σ and V estimated at the beginning of deformation is demonstrated in figure 2 [20, 21]. The flow stress is almost independent of temperature up to about 1000 K and then decreases. In contrast $1/V$ passes through a broad minimum between 800 and 1000 K indicating that significant changes in the micromechanisms controlling the dislocation velocity occur. The relevant processes have been investigated in several studies. Accordingly, at room temperature the dislocation velocity is controlled by a combined operation of localized pinning, jog dragging and lattice friction [3, 20], while locking of dislocations due to the formation of defect atmospheres occurs in the temperature range 420 to 770 K [22, 23]. There is increasing evidence that the defect atmospheres in two-phase alloys are formed by antisite defects, i. e. Ti atoms situated on Al sites [24]. The strong increase of the reciprocal activation volume above 900 K indicates that a new thermally activated process becomes important. For the materials investigated here this temperature is just the brittle ductile transition, where the flow stress degrades. In most cases, the activation enthalpy is close to 3 eV [3, 20, 21], which is in reasonable agreement with the self-diffusion energy of $\gamma(\text{TiAl})$ [25]. This is indication of a diffusion assisted dislocation mechanism. Climb of ordinary $1/2\langle 110 \rangle$ dislocations has been recognized on different γ -base titanium aluminide alloys by post mortem [26] and in situ TEM studies [3, 20]. Dislocation climb is known to be a stress driven thermally activated process. Thus, the strength properties of the material become strongly rate dependent and degrade at low strain rates. These features are also characteristic of the high temperature deformation of the titanium aluminides and particularly harmful for their creep resistance. An important point is the observation that the activation enthalpy ΔH of the alloys containing a large addition of Nb (alloy 4-6) [21] is significantly higher than that of other alloys. The result implies that diffusion assisted deformation

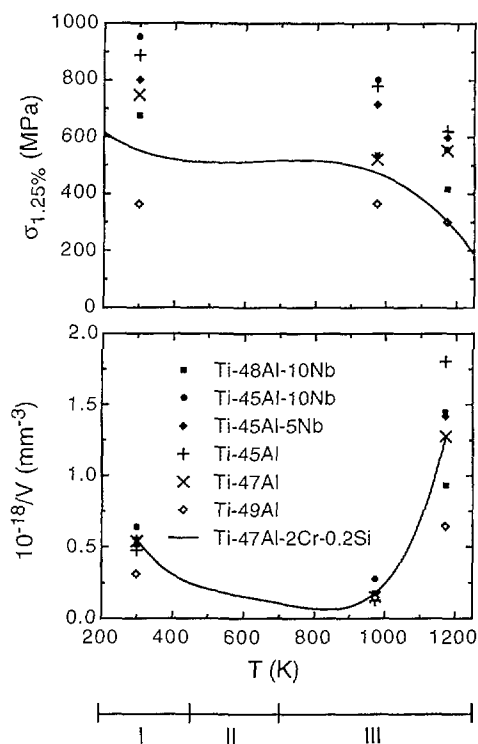


Figure 2. Dependence of the flow stress σ and the reciprocal activation volume $1/V$ of binary and niobium containing alloys on the deformation temperature. The drawn lines refer to the values of a Ti-47Al-2Cr-0.2Si alloy with a near γ microstructure. Values estimated at strain $\varepsilon = 1.25\%$ and strain rate $\dot{\varepsilon} = 4.16 \times 10^{-4} \text{ s}^{-1}$.

processes are impeded by Nb additions, which might be beneficial for the design of creep resistant TiAl alloys [21].

3. Creep Properties:

For the intended applications γ (TiAl)-base should have a good creep resistance, which must be present in the earlier stages of deformation. As with other mechanical properties the creep characteristics are sensitive to alloy

composition and microstructure and considerable improvements have been achieved by optimizing these two factors [27]. Much emphasis has been placed on describing the stress and temperature dependence of the creep rate in terms of the Dorn equation [28]. While differences in the details of interpretation are common, there has been general agreement about the fact that creep of fully-lamellar materials at moderately low stresses ($\sigma \leq 150$ MPa) and temperatures ($T < 750$ °C) is controlled by climb of ordinary dislocations. However, rather less is known about the micromechanisms controlling low creep rates, which apparently are more relevant for engineering applications. This imbalance of information will be addressed in the present section in that electron microscope observations performed after long-term creep will be discussed [29-32]. Among the various microstructures that can be established in two-phase alloys fully-lamellar structures exhibit the best creep resistance, and, thus, will be mainly considered here.

The alloy investigated had the composition (in at.%) Ti-48Al-2Cr, which might be considered as a model alloy for fully-lamellar materials. Tensile samples were crept for 6.000 to 13.400 hours at 700 °C and stresses ranging between 80 and 140 MPa [29-32]. After creep testing the materials were found to have undergone significant microstructural changes. A prominent feature is the formation of multiple-height ledges perpendicular to the interfacial boundaries (figure 3). The ledges had often grown into zones which extended over about 10 nm.

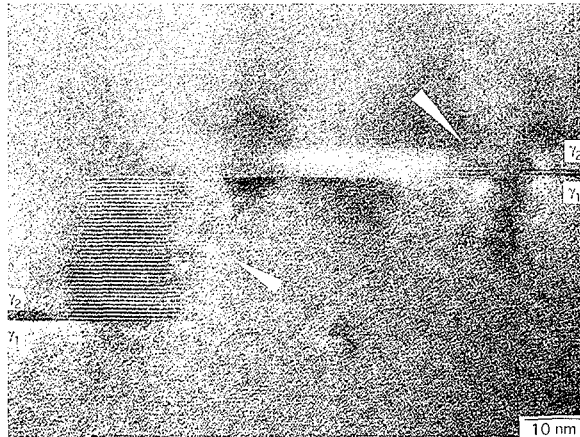


Figure 3. Structural changes observed after long-term creep of a Ti-48Al-2Cr alloy at $T = 700$ °C, stress $\sigma_a = 140$ MPa, $t = 5.988$ hours to strain $\epsilon = 0.69$ %. Note the formation of extended ledges at a γ/γ interface.

The formation of these ledges can formally be rationalized by twinning and antitwinning operations parallel to the (111) plane of the interfaces [32]. When the slabs grow further it is apparently energetically favorable to nucleate a γ grain. Two-phase alloys with the base line composition Ti-(45-48)Al-2Cr suffer from dissolution of the α_2 phase and coarsening of the γ lamellae. This is because the kinetics of the decomposition of the α phase into α_2 and γ lamellae during cooling after processing is sluggish and the volume fraction of gamma is less than at equilibrium. Thus, during long term creep, dissolution of the α_2 phase and formation of γ grains occur and finally lead to a complex conversion of the lamellar morphology to a fine spheroidized microstructure. There is ample evidence that misfit dislocations and interface ledges play an important role for achieving the phase equilibrium in that they provide the required change in the stacking sequence and serve as paths for easy diffusion. More on this subject is provided in separate studies [30, 31]. In view of these observations an alloy design towards improved high temperature strength and creep resistance should rely on systems with stable phases and microstructures. Equally important are a reduced diffusivity of the material and the implementation of additional glide resistance, in order to impede dislocation climb processes.

4. Alloy Design towards Improved Strength:

In view of the anticipated applications several studies have been performed in order to strengthen γ (TiAl) base alloys by solid solution and precipitation hardening. From the engineering viewpoint the challenge is to establish these mechanisms without compromising desirable low-temperature properties, such as ductility and toughness.

Recently, it has been shown that a significant strengthening effect can be achieved when Nb is added with an amount of 5-10 at.% to polycrystalline two-phase alloys [21, 33, 34]. Nb is also a commonly added element because of its ability to improve the oxidation resistance [35, 36]. Despite the extensive body of investigations broadly confirming these results, there is some controversy about the nature of the strengthening effect of Nb additions, i. e. whether or not it arises from solid solution hardening. Thus, the origin of the hardening mechanism has been studied by a systematic variation of the Al and Nb contents. The investigations involve tests on binary alloys with the equivalent Al contents, which are thought to ascertain the effects of off-stoichiometric deviations on microstructure and yield strength [21]. As dem-

onstrated in figure 2 the strengthening effect is almost independent of the Nb content and the values of the reciprocal activation volume estimated for the binary alloys are very similar to those of the Nb containing alloys. Thus, the strengthening effect of large Nb additions has been attributed to the related changes of the microstructure. This view is supported by recent ALCHEMI studies (atom location by channeling enhanced microanalysis) of site occupation, which revealed that Nb solely occupies the Ti sublattice [37, 38]. However, the Nb containing alloys exhibit at room temperature an appreciable ductility, whereas the binary alloys of the same Al content do not. This finding indicates that significant changes of the deformation mechanism occurred due to the Nb additions. In Nb containing alloys an abundant activation of twinning has been recognized and the superdislocations were found to be widely dissociated. As planar faults, twins and dissociated superdislocations often coexist in the same grain or lamella, it is speculated that the stacking fault energies of $\gamma(\text{TiAl})$ are lowered by the Nb additions and that twin nucleation originates from the superposition of extended stacking faults on alternate $\{111\}$ planes [15, 39].

Appreciable improvements in strength and creep resistance have also been achieved by precipitation hardening [40, 41]. The strengthening effect critically depends on the size and the dispersion of the particles. In this respect carbides, nitrides and silicides appear to be beneficial as the optimum dispersion can be achieved by homogenization and ageing procedures. Utilizing this method, in a Ti-48.5Al-0.37C alloy a fine dispersion of Ti_3AlC precipitates were generated which is characterized by a length $l_p=22$ nm and width (along $\langle 100 \rangle$) $d_p=3.3$ nm of the precipitates [41]. The precipitates are elongated along the c axis of the γ matrix and exhibit strong coherency stresses due the differences in crystal structure and lattice constants. These structural features give rise to a strong glide resistance for all types and characters of dislocations, which persists up to temperatures of about 750 °C and leads to significantly improved high temperature strength and creep resistance. Figure 4 demonstrates, e.g., the interaction of deformation twins with the precipitates in some detail [41]. The high glide resistance is manifested by the strong bowing-out of the twinning partial dislocations. In the local region of the precipitates the shape of the twin/matrix interface is much less regular and the twins are often deflected. These processes often lead to fragmentation of the twins, i.e. islands of untwinned regions occur. However, as with the TiAl-Nb alloys, twin nucleation seems to be relatively easy. Twin nuclei were often found together with widely separated superdislocations giving rise to the speculation that the twins originate from overlapping stacking faults [15]. In

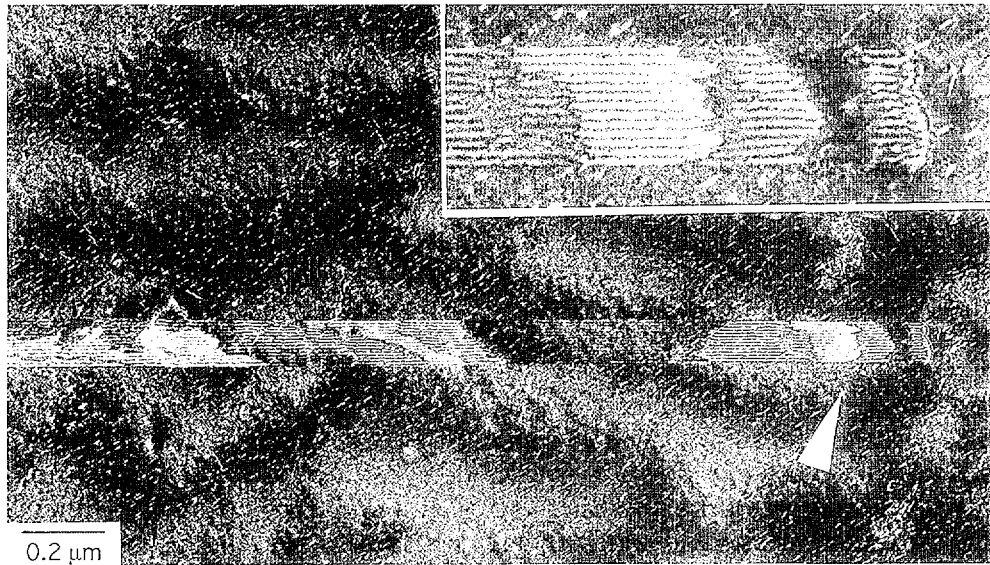


Figure 4. Immobilization of a deformation twin due to the interaction with Ti_3AlC perovskite precipitates. Note the high density of the precipitates, which become evident by strain contrast, and the pinning of the twinning partial dislocations by the precipitates. Ti-48.5Al-0.37C, compression at $T = 300$ K to strain $\epsilon = 3$ %.

this way a fine dispersion of deformation twins is formed, which provides shear components in c direction of the tetragonal cell of $\gamma(TiAl)$ and, thus, is beneficial for room temperature ductility and toughness.

However, carbides and nitrides seem to be susceptible to coarsening by Ostwald ripening, thereby reducing their effectiveness in impeding dislocation motion. In case of carbides implementation of H phase particles Ti_2AlC could be a possible alternative [40], because this phase is thermodynamically more stable and apparently provides also a good creep resistance. However, coarse platelets of H-phase tend to be located at lamellar colony boundaries, which is certainly harmful for low temperature ductility. Borides are virtually stable up to the melting point of $\gamma(TiAl)$, however, metallurgical techniques to refine their relatively coarse dispersion appear to be less efficient.

Nevertheless, in conclusion of this section it may be summarized that an alloy design based on relatively large Nb additions together with a fine dispersion

of perovskite or H-phase precipitates seems to be a suitable technique for expanding the service range for titanium aluminides towards higher temperatures and stresses.

5. Processing:

γ (TiAl) alloys are available in all conventional product forms: ingot forgings, extrusions and sheet. The structural applications outlined in the introductory section may require the material to be formed into complex geometries with large dimensions. Processing routes generally follow those of conventional titanium alloys with some special alterations. Yet titanium aluminides are generally difficult to process due to their solidification behaviour, susceptibility to degradation from contamination and intrinsic brittleness. This holds particularly for the novel high strength material described in the previous section, for which the hardening mechanisms have to be implemented within the constraints of technically acceptable processing routes. In view of the available coverage of this article attention is concentrated on ingot metallurgy and wrought processing.

5.1 Ingot quality:

Vacuum arc melting (VAR) is currently the most widely used practice for preparing ingots from elemental or master alloying additions. In order to ensure a reasonable chemical homogeneity throughout ingots of 200 -300 mm diameter the meltstocks are usually double-or triple-melted [42]. The peritectic solidification reactions occurring in the composition range (45-49) at.% Al give rise to an unavoidable micro-segregation, the extent of which depends on the nominal Al level and the content of refractory elements. Al is rejected to the interdendritic region while refractory elements, in particular those stabilizing the β phase, are concentrated in the dendritic cores. The differences in concentration are as large as a few at.% and vary on a length scale of about 1 mm [43]. Rapid solidification processing generally reduces segregation, refines microstructure and, thus, produces a more homogeneous material consolidation. As ingot size increases, cooling becomes slower and the as-cast grain size increases, thereby exacerbating the problems associated with segregation. Heat treatments in the $(\alpha+\gamma)$ phase field are mostly ineffective to mitigate the chemical gradients [44, 45]. Annealing in the α or $(\alpha+\beta)$ phase

fields lead to significantly faster homogenization kinetics, but mostly results in rapid grain growth.

5.2 Primary ingot break-down:

Significant improvements in the chemical homogeneity and refinement of microstructure can be achieved by hot working and the associated dynamic recrystallization. There is an intimate correlation between alloy chemistry, hot working conditions and the evolution of the microstructure, which has to be considered for the alloy design and processing. The microstructural evolution has been systematically studied on a series of binary and technical alloys with aluminium contents ranging between 45 and 54 at. % [46]. Not surprisingly, the degree of dynamic recrystallization increases with strain, however, no substantial recrystallization occurs below strains of about 10%. There is also a marked effect of the aluminium concentration on the recrystallization behaviour, which is manifested in the observation that the recrystallized volume fraction is at maximum for aluminium contents of 48-50 at.% (figure 5). The recrystallization behaviour of two-phase alloys is also supported by the presence of boride particles [46]. Boron is known to significantly refine the as-cast microstructure, which is generally a good precondition for homogeneous hot working and recrystallization [6]. In addition, particle stimulated dynamic recrystallization may occur, when dislocations are accumulated at the particles during hot working [46].

Primary ingot break-down has been accomplished on an industrial scale utilizing forging and extrusion [1, 5, 43-53]. Typical conditions for large-scale isothermal forging are $T=1000-1200^{\circ}\text{C}$ at strain rates $\dot{\epsilon} = 10^{-3} - 10^{-2} \text{ s}^{-1}$. 50 kg-billets have been successfully forged within this processing window to height reductions of 5:1. The as-forged structure appears banded, consisting of stringers of α_2 particles in a fine grained γ matrix. In two-phase alloys it is also common to observe lamellar colonies with lamellae lying in the plane of forging. These colonies are probably undeformed remnants from the cast structure.

Extrusion is usually carried out at temperatures around the α -transus temperature [1, 5, 49, 51-53]. Under these conditions (typically $1250 - 1380^{\circ}\text{C}$) severe oxidation and corrosion occurs, thus, the work piece has to be encapsulated. In most cases conventional Ti alloys or austenitic steels are used as can material. At the extrusion temperature the can materials have a significantly lower flow stress than the TiAl billet [54]. This flow stress mismatch is

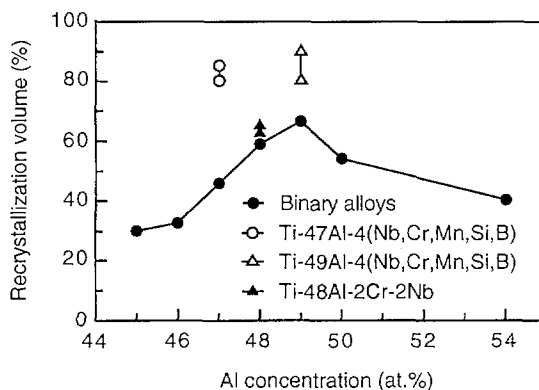


Figure 5. Dependence of the volume fraction of recrystallized grains on the aluminium content of binary and technical alloys [46]. Deformation at $T = 1000\text{ }^{\circ}\text{C}$ and $\dot{\epsilon} = 5 \times 10^{-4}\text{ s}^{-1}$ to strain $\epsilon = 75\%$.

often as high as 300 MPa and leads to inhomogeneous extrusion and cracking. These problems can largely be overcome by a novel can design involving radiation shields as an effective thermal insulation [55]. This reduces the heat transfer from the work piece to the can and enables controlled dwell periods between preheating and extrusion. Taking advantage of this concept, extrusion processes have been widely utilized for TiAl ingot break down. For example, 80 kg ingots were uniformly extruded into a rectangular shape with a reduction of the cross section of 10:1 (figure 6) [43]. The alloy had the composition Ti-45Al-10Nb and represents a new family of high strength materials that have been described in the previous section. Extrusion above the T_{transus} resulted in a refined nearly-lamellar microstructure with a colony size of 30-50 μm as demonstrated in figure 7a. Extrusion below T_{transus} led to duplex microstructures with coarse and fine-grained banded regions (figure 7b). These structural inhomogeneities are associated with a significant variation in the local chemical composition, which is manifested at a length scale comparable to or slightly smaller than that of the as-cast material [43]. This observation provides supporting evidence that the dynamic recrystallization during hot working is strongly affected by local composition. The coarse-grained bands probably originate from the prior Al-rich interdendritic regions where no β_2 phase was present. Thus, grain growth following recrystallization is not impeded by β_2 grains. On contrary, the fine-grained bands or lamellar colonies are formed in Al-depleted core regions of the dendrites.

The structural and chemical inhomogeneities of primarily processed TiAl products provide severe limitations for the reliability of components or secondary processing. Other quality issues concern cavities, internal wedge cracks and surface connected cracks. Thus, further improvement of hot working procedures is of major concern. In view of the results discussed above, this re-

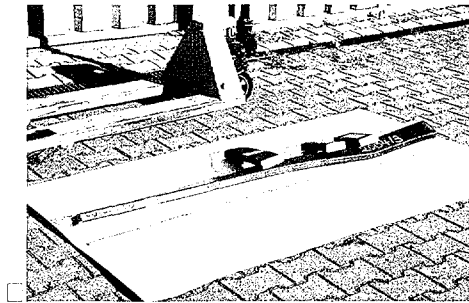


Figure 6. Ingot break-down of an engineering alloy with the base line composition Ti-45Al-(5-10)Nb+X by canned extrusion at $T_{\alpha-\Delta T}$. The ingot, originally of 192 mm diameter and 700 mm height, was canned using austenitic steel, sealed in vacuum, heated up and then extruded. A reduction ratio of 10:1 and a rectangular die were used. The final TiAl extrusion was rectangular with cross section dimensions of 100 x 30 mm².

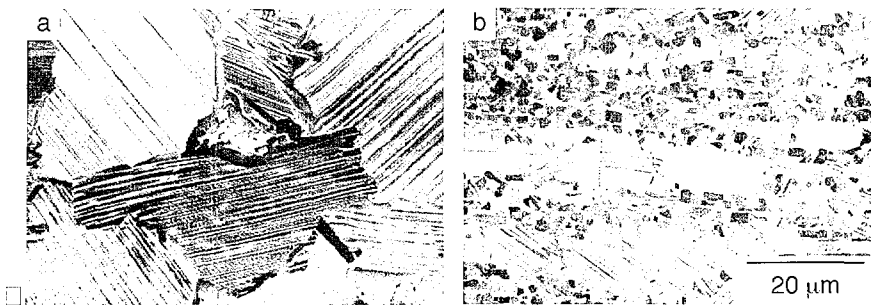


Figure 7. Back-scattered electron images of a Ti-45Al-10Nb alloy extruded to 7:1 reduction. (a) Nearly lamellar microstructure observed after extrusion at $T_{\alpha-\Delta T}$. (b) Duplex structure with a banded morphology observed after extrusion at $T_{\alpha-\Delta T}$.

quires a tight optimization of the alloy composition and hot working parameters, respectively, and to find novel engineering solutions for increasing the amount of imparted strain energy, in order to achieve a more homogeneous recrystallization. Advances in the manufacturing of components have been described in recent conference proceedings and review articles [1, 2, 5, 43, 44, 52, 56], the reader is referred to these papers for further details.

5.3 Mechanical properties of wrought material:

The refined microstructure established after hot working generally results in a significant strengthening, when compared with cast material. The increase in yield strength can be rationalized in terms of Hall-Petch relations although quantitative descriptions are often difficult due to the complexity of the microstructures [57]. Figure 8 shows the dependence of the density compensated yield stress on temperature for forged and extruded γ base alloys, which have been developed at GKSS. Extremely high yield stresses in excess of 1000 MPa were obtained on Ti-45Al-(5-10)Nb derivative alloys after extrusion to a reduction ratio of 7:1 [43]. For example on one alloy variant (figure 8) at room

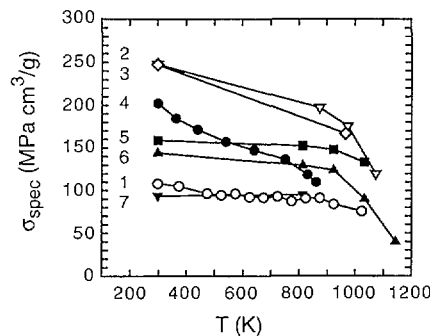


Figure 8. Temperature dependence of density adjusted yield stresses for forged and extruded gamma-base titanium aluminide alloys. (1) Forged Ti-47Al-2Cr-0.2Si, near gamma microstructure, (2) extruded Ti-45Al-(5-10)Nb, duplex microstructure, (3) Ti-45Al-(5-10)Nb+X, duplex microstructure. For comparison the values of nickel base superalloys and conventional titanium alloys are given, with (4) IMI 834, (5) René 95, (6) Inconel 718, (7) IN 713 LC.

temperature in tension a fracture stress of 1100 MPa at a plastic strain of $\epsilon=2.5\%$ was determined. This combination of room temperature strength and ductility is the best ever reported on $\gamma(\text{TiAl})$ base alloys.

Conclusions:

During the past five years significant progress has been achieved in the physical metallurgy of titanium aluminide alloys. Compositions of alloys have been identified that are capable of carrying stresses in excess of 900 MPa at service temperatures of 700°C. Thus, wrought alloys of this type can be an attractive alternative to the heavier nickel base superalloys in certain ranges of stress and temperature. The future and promise of $\gamma(\text{TiAl})$ base alloys and manufacturing of components lies in innovative processing methods designed to achieve better performance. Specifically, substantial improvements are required in ingot quality and hot working procedures to obtain homogeneous and defect-free material with desired microstructures.

Acknowledgements:

The authors would like to thank Ms. E. Tretau, U. Brossmann, U. Christoph, St. Eggert, U. Lorenz, J. Müllauer, and J. Paul for helpful discussions and continuous support. The financial support of this research by the Helmholtz-Gemeinschaft (HGF-Strategiefonds) is gratefully acknowledged.

References:

1. Y-W. Kim and D.M Dimiduk, *Structural Intermetallics*, eds. M. V. Nathal, R. Darolia, C. T. Liu, P. L. Martin, D. B. Miracle, R. Wagner, M. Yamaguchi, (TMS, Warrendale, PA, 1997), p. 531.
2. *Gamma Titanium Aluminides 1999*, eds. Y-W. Kim, D. M. Dimiduk, M. H. Loretto, (TMS, Warrendale, PA, 1999).
3. F. Appel and R. Wagner, *Mater. Sci. Eng.* **R22**, 187-268, 1998.
4. M. Yamaguchi, H. Inui, K. Itoh, *Acta Mater.* **48**, 307 (2000).
5. H. Clemens, H. Kestler, *Advanced Eng. Mater.* **2**, 551 (2000).

6. J. A. Christodoulou, H. M. Flower, *Advanced Eng. Mater.* **2**, 631 (2000).
7. D. M. Dimiduk, *Mater. Sci. Eng.* **A263**, 281 (1999).
8. M. Yamaguchi and Y. Umakoshi, *Progress in Materials Science* **34**, 1-148 (1990).
9. K. J. Hemker, B. Viguier and M. J. Mills, *Mater. Sci. Eng.* **A164**, 391 (1993).
10. J. P. Hirth and J. Lothe, *Theory of Dislocations*, 2nd edn. (Krieger Publishing, Malabar), (1992).
11. F. Appel, U. Christoph and R. Wagner, *Phil. Mag. A* **72**, 341 (1995).
12. F. Appel, P. A. Beaven and R. Wagner, *Acta Metall. Mater.* **41**, 1721 (1993).
13. F. Appel, U. Christoph and R. Wagner, *Interface Control of Electrical, Chemical and Mechanical Properties*, eds. S. P. Murarka, K. Rose, T. Ohmi, and T. Seidel, Mater. Res. Soc. Symp. Proc. (MRS, Pittsburgh, PA, 1994), Vol. **318**, p. 691.
14. F. Appel and U. Christoph, *Intermetallics* **7**, 1273 (1999).
15. F. Appel, in *Advances in Twinning*, eds. S. Ankem and C. S. Pande (TMS, Warrendale, PA, 1999), pp. 171-186.
16. M. H. Yoo, C. L. Fu, J.K. Lee, *Twinning in Advanced Materials* (TMS, Warrendale, PA, 1994), p. 97.
17. M. H. Yoo, C. L. Fu, *Metall. Trans. A*, **29A**, 49 (1998).
18. G. Schöck, *Phys. Stat. Sol.* **8**, 499 (1965).
19. G. Evans and R. W. Rawlings, *Phys. Stat. Sol.* **34**, 9 (1969).
20. F. Appel, U. Lorenz, M. Oehring, U. Sparka and R. Wagner, *Mater. Sci. Eng.* **A233**, 1 (1997).
21. J. D. H. Paul, F. Appel and R. Wagner, *Acta Mater.* **46**, 1075 (1998).
22. M. A. Morris, T. Lipe and D. G. Morris, *Scripta Mater.* **34**, 1337 (1996).
23. U. Christoph, F. Appel and R. Wagner, *High-Temperature Ordered Intermetallics VII*, eds. C.C. Koch, C.T. Liu, N.S. Stoloff, A. Wanner, Mater. Res. Soc. Symp. Proc. (MRS, Pittsburgh, PA, 1997), Vol. 460, p. 77.
24. U. Christoph, F. Appel, this volume.
25. S. Kroll, H. Mehrer, N. Stolwijk, Ch. Herzig, R. Rosenkranz and G. Frommeyer, *Z. Metallkunde* **83**, 8 (1992).

26. K. Kad and H. L. Fraser, *Phil. Mag. A*, **69**, 689 (1994).
27. J. Beddoes, W. Wallace and L. Zhao, *International Materials Reviews* **40**, 197 (1995).
28. T.A. Parthasaraty, M.G. Mendiratta and D.M. Dimiduk, *Scripta Mater.* **37**, 315 (1997).
29. M. Oehring, P.J. Ennis, F. Appel and R. Wagner, *High-Temperature Ordered Intermetallics VII*, Mater. Res. Soc. Symp. Proc. (MRS, Pittsburgh, PA 1997), Vol. 460, p. 257.
30. M. Oehring, F. Appel, P. J. Ennis and R. Wagner, *Intermetallics 7*, 335 (1999).
31. F. Appel, M. Oehring and P. J. Ennis, *Gamma Titanium Aluminides 1999*, eds. Y.-W. Kim, D. M. Dimiduk, M. H. Loretto (TMS, Warrendale, PA, 1999), p.603.
32. F. Appel and R. Wagner, *Atomic Resolution Microscopy of Surfaces and Interfaces* ed. D.J.Smith, Mater. Res. Soc. Symp. Proc. (MRS, Pittsburgh, PA, 1997),Vol. 466, p. 145.
33. S.-C. Huang, *Structural Intermetallics* , eds. R. Darolia, J. J. Lewandowski, C. T. Liu, P. L. Martin, D. B. Miracle, M. V. Nathal (TMS, Warrendale, PA, 1993), p. 299.
34. G. Chen, W. Zhang, Y. Wang, J. Wang and Z. Sun, *Structural Intermetallics*, eds. R. Darolia, J. J. Lewandowski, C. T. Liu, P. L. Martin, D. B. Miracle, M. V. Nathal (TMS, Warrendale, PA, 1993), p. 319.
35. H. Nickel, N. Zheng, A. Elschner and W. Quadakkers, *Microchim. Acta* **119**, 846 (1995).
36. L. Singheiser, W.J. Quadakkers and V. Shemet, *Gamma Titanium Aluminides 1999* , eds. Y-W. Kim, D. M. Dimiduk, M. H. Loretto (TMS, Warrendale, PA, 1999), p. 743.
37. E. Mohandas and P. A. Beaven, *Scripta Metall. Mater.* **25**, 2023 (1991).
38. J. Rossouw, C. T. Forwood, M. A. Gibson and P. R. Miller, *Phil. Mag. A* **74**, 77 (1996).
39. F. Appel, U. Lorenz, J.D.H. Paul and M. Oehring, *Gamma Titanium Aluminides 1999*, eds. Y.-W. Kim, D. M. Dimiduk, M. H. Loretto (TMS, Warrendale, PA, 1999), p. 381.
40. W.H. Tian and M. Nemoto, *Gamma Titanium Aluminides*, eds. Y-W. Kim, R. Wagner and M. Yamaguchi (TMS, Warrendale, PA, 1995), p. 689.

41. U. Christoph, F. Appel and R. Wagner, *Mater. Sci. Eng.* **A239-240**, 39 (1997).
42. P. McQuay, V.K. Sikka, *Intermetallic Compounds*, Vol. 3, Progress, eds. J.H. Westbrook, R.L. Fleischer (J. Wiley, Chicester, 2001), in press.
43. F. Appel, U. Brossmann, U. Christoph, S. Eggert, P. Janschek, U. Lorenz, J. Müllauer, M. Oehring, J. D. H. Paul, *Adv. Eng. Mater.* **2**, 699 (2000).
44. S. L. Semiatin, J. C. Chesnutt, C. Austin, V. Seetharaman, *Structural Intermetallics 1997*, eds. M. V. Nathal, R. Darolia, C. T. Liu, P. L. Martin, D. B. Miracle, R. Wagner, M. Yamaguchi (TMS, Warrendale, PA, 1977), p. 263.
45. Koeppe, A. Bartels, J. Seeger and H. Mecking, *Metall. Trans.* **24A**, 1795 (1993).
46. R. M. Imayev, G. A. Salishchev, V. M. Imayev, M. R. Shagiev, A. V. Kuznetsov, F. Appel, M. Oehring, O. N. Senkov, F. H. Froes, *Gamma Titanium Aluminides 1999*, eds. Y-W. Kim, D. M. Dimiduk, M. H. Loretto (TMS, Warrendale, PA, 1999), p. 565.
47. Y-W. Kim, *Acta Metall. Mater.* **40**, 1121 (1992).
48. R.M. Imayev, V.M. Imayev and G.A. Salishchev, *J. Mater. Sci.* **27**, 4465 (1992).
49. P.L. Martin, C.G. Rhodes and P.A. McQuay, *Structural Intermetallics*, eds. R. Darolia, J.J. Lewandowski, C.T. Liu, P.L. Martin, D.B. Miracle, and M.V. Nathal (TMS, Warrendale, PA, 1993), p. 177.
50. H. Clemens, P. Schretter, K. Wurzwallner, A. Bartels and C. Koeppe, *Structural Intermetallics*, eds. R. Darolia, J.J. Lewandowski, C.T. Liu, P.L. Martin, D.B. Miracle, and M.V. Nathal (TMS, Warrendale, PA, 1993), p. 205.
51. C.T. Liu, P.J. Maziasz, D.R. Clemens, J.H. Schneibel, V.K. Sikka, T.G. Nieh, J. Wright and L.R. Walker, *Gamma Titanium Aluminides*, eds: Y-W. Kim R. Wagner, M. Yamaguchi (TMS, Warrendale, PA, 1995), p. 679.
52. H. Clemens, H. Kestler, N. Eberhardt, W. Knabl, *Gamma Titanium Aluminides 1999*, eds. Y-W. Kim, D. M. Dimiduk, M. H. Loretto (TMS, Warrendale, PA, 1999), p. 209.

53. M. Oehring, U. Lorenz, R. Niefanger, U. Christoph, F. Appel, R. Wagner, H. Clemens and N. Eberhardt, *Gamma Titanium Aluminides 1999*, eds. Y-W. Kim, D. M. Dimiduk, M. H. Loretto (TMS, Warrendale, PA, 1999), p. 439.
54. S.L. Semiatin and V. Seetharaman, *Scripta Metall. Mater.* **31**, 1203 (1994).
55. Of patent application by F. Appel, U. Lorenz, M. Oehring and R. Wagner, DE 1974257A1, FR Germany.
56. H. Clemens, A. Lorich, N. Eberhardt, W. Glatz, W. Knabl, H. Kestler, Z. Metallkde. **90**, 569 (1999).
57. M. Dimiduk, P. M. Hazzledine, T. A. Parthasarathy, S. Seshagiri, M. G. Mendiratta, *Metall. Trans. A*, **29** (1998), 37.